

Structural study of $(\text{Se}_{80}\text{Te}_{20})_{100-x}\text{Ag}_x$ bulk samples using XRD spectra: Applicability of Piloyan–Borchardt method

DIGVIJAY SINGH, SANDEEP KUMAR, R. THANGARAJ*

Semiconductors Laboratory, Department of Physics, Guru Nanak Dev University, Amritsar-143005, Punjab, India

The XRD analysis has been carried out on pristine and annealed bulk samples of $(\text{Se}_{80}\text{Te}_{20})_{100-x}\text{Ag}_x$ ($1 \leq x \leq 4$) glassy system. XRD traces of all the samples have been taken out at the room temperature. The absence of the sharp peaks in the pristine bulk samples confirmed the amorphous nature but the presence of sharp peaks in the XRD pattern of annealed samples confirmed the presence of Se_8 and Ag_5Te_3 phase in the bulk material. The particle size has been calculated by the Scherrer's formula and found to be in the range of 0.008277 μm to 0.038694 μm . Activation energy of crystallization of glassy system has been obtained by Piloyan-Borchardt method for both phases at different x values as well as at different heating rates. It has been found that the value of activation energy of crystallization is highest for $x=3$ and lowest for $x=1$.

(Received October 9, 2010; accepted November 19, 2010)

Keywords: XRD, Average particle size. Se-Te-Ag system

1. Introduction

Chalcogenide materials are widely studied for their potential applications in active as well as passive solid-state electronics and optical devices. The applications include photoreceptor in xerography [1], optical recording and memory switching [2, 3], infrared optical fibers and waveguides [4] and non-linear optics [5]. Chalcogenide glasses are based on the chalcogen elements S, Se and Te but not O. Selenium is considered to be one of the most important semiconductors due to its unusual structure [6] and it exhibits the unique property of reversible phase transformation [7]. It has the wide commercial applications like switching, memory and xerography which make it attractive. But in the pure state it has the disadvantages of short lifetime and low sensitivity and low thermal instability. This problem can be removed by alloying Se with some impurity atoms which gives higher sensitivity, higher crystallization temperature and smaller ageing effects [8-10]. It has been pointed out that addition of Te to Se improves the corrosion resistance [11] and lengthens the crystallization time of amorphous selenium [12]. Glassy alloys of the Se-Te system based on selenium have become materials of considerable commercial importance and are widely used for optical recording media because of their excellent laser writing sensitivity [13] but these advantages depend on material stability [14]. The Se-Te alloys have been found to be useful from the technological point of view due to their greater hardness, higher crystallization temperature T_c , and smaller ageing effects as compared to a-Se [15]. Experimental results indicate that the properties of the Se-Te alloys are highly composition dependent. Addition of Ag will expand the glass forming area and also create compositional and configurational disorder in the system and has large effect on their structural, physical, optical,

electronic and thermal properties [16]. In the present work, the structural studies of $(\text{Se}_{80}\text{Te}_{20})_{100-x}\text{Ag}_x$ glassy system have been carried out by analysing the XRD traces of the annealed bulk samples. Various properties like particle size (t), lattice parameters (a, b, c), miller indices (h, k, l) are also observed. The activation energy of crystallization is calculated by the Piloyan–Borchardt method.

2. Experimental

Bulk samples of $(\text{Se}_{80}\text{Te}_{20})_{100-x}\text{Ag}_x$ ($1 \leq x \leq 4$) were prepared by conventional melt quenching technique. High-purity (99.999%) elements with appropriate atomic percentage were sealed in a quartz ampoule (length ~100mm and internal diameter ~6mm) in a vacuum of 10^{-5} mbar. The ampoules were kept inside a vertical furnace for 72 h. The temperature was raised to 1373K, at a rate of 4-5 K/min. The ampoule was inverted at regular intervals of time to ensure homogeneous mixing of the constituents. The ampoule was then quenched in ice-cold water. The bulk material was separated from the quartz ampoule by dissolving the ampoule in $\text{HF}+\text{H}_2\text{O}_2$ solution for approximately 48 h. The amorphous nature of the bulk samples was confirmed by the absence of sharp peaks in the X-ray diffractogram. XRD studies were done using Phillips PAN ANALYTICAL machine and X-ray of Cu K_α line to check the amorphous nature of the materials. About one gram of bulk samples of $(\text{Se}_{80}\text{Te}_{20})_{100-x}\text{Ag}_x$ ($1 \leq x \leq 4$) have been annealed at 348K and 398K at heating rate of 4-5K/min in the vacuum of 10^{-5} mbar to know about the evolution of different crystalline phases in the material. Using this material, thin films were deposited onto chemically cleaned glass substrates by thermal evaporation technique in a vacuum of 10^{-5} mbar using a Hind High Vacuum coating unit (model 12A4D). The

thermal behaviour of the samples was investigated using Perkin Elmer (Pyris Diamond) DSC System. DSC runs were taken for four different heating rates i.e., 5, 10, 15 and 20 K/min for each of the composition so as to get glass transition temperature (T_g), crystallization temperature (T_c), peak crystallization temperature (T_p) and melting temperature (T_m). The fraction α_c crystallized at a temperature T was calculated using the relation $\alpha_c = A_T/A$ where A is the total area of the exotherm between T_c and the temperature at which crystallization is completed, A_T is the area between T_c and T . DSC thermograms of $(\text{Se}_{80}\text{Te}_{20})_{100-x}\text{Ag}_x$ ($0 \leq x \leq 4$) glassy alloys at different x values and at different heating rates along with deconvoluted peaks are shown elsewhere [17].

3. Results

3.1 Analysis of XRD spectra of annealed $(\text{Se}_{80}\text{Te}_{20})_{100-x}\text{Ag}_x$ ($1 \leq x \leq 4$) bulk materials

Fig. 1 shows the XRD spectra of the pristine bulk samples of $(\text{Se}_{80}\text{Te}_{20})_{100-x}\text{Ag}_x$ ($1 \leq x \leq 4$) system. The absence of the sharp peaks indicates that the material is amorphous in the nature. The XRD spectra of the bulk samples annealed at 348K show the presence of Se_8 crystalline phase in the material, but the bulk samples annealed at the 398K shows the presence of Se_8 as well as Ag_5Te_3 phase. The XRD spectra of annealed bulk samples of $(\text{Se}_{80}\text{Te}_{20})_{100-x}\text{Ag}_x$ ($1 \leq x \leq 4$) is shown elsewhere [17].

Table 1. Various structural parameters of annealed $(\text{Se}_{80}\text{Te}_{20})_{100-x}\text{Ag}_x$ ($1 < x < 4$) system.

Composition	Crystal Phase	2θ	$\cos\theta$	h,k,l	d	B(rad)	Particle size (um)	Crystal structure	T(K)
$(\text{Se}_{80}\text{Te}_{20})_{99}\text{Ag}_1$	Se_8	23.472	0.9790	3,2,1	3.8162	0.004848	0.029211	Monoclinic	Annealed at 348K
$(\text{Se}_{80}\text{Te}_{20})_{98}\text{Ag}_2$	Se_8	18.472	0.9870	0,2,2	3.7671	0.012120	0.011590	Monoclinic	
$(\text{Se}_{80}\text{Te}_{20})_{97}\text{Ag}_3$	Se_8	18.680	0.9867	0,2,2	3.7702	0.014544	0.009661	Monoclinic	
$(\text{Se}_{80}\text{Te}_{20})_{96}\text{Ag}_4$	Se_8	18.402	0.9871	0,2,2	3.7602	0.016968	0.008277	Monoclinic	
$(\text{Se}_{80}\text{Te}_{20})_{99}\text{Ag}_1$	Se_8	23.541	0.9789	1,2,1	3.8391	0.009696	0.014674	Monoclinic	Annealed at 398K
	Ag_5Te_3	29.236	0.9676	2,1,1	3.9102	0.008484	0.016889	Hexagonal	
$(\text{Se}_{80}\text{Te}_{20})_{98}\text{Ag}_2$	Se_8	18.611	0.9868	2,2,1	3.0822	0.003631	0.038694	Monoclinic	
	Ag_5Te_3	22.891	0.9801	2,1,2	3.0581	0.007272	0.019452	Hexagonal	
$(\text{Se}_{80}\text{Te}_{20})_{97}\text{Ag}_3$	Se_8	18.819	0.9865	2,2,1	3.0862	0.006060	0.023191	Monoclinic	
	Ag_5Te_3	22.916	0.9800	3,1,1	3.023	0.013332	0.010611	Hexagonal	
$(\text{Se}_{80}\text{Te}_{20})_{96}\text{Ag}_4$	Se_8	18.607	0.9868	2,2,1	3.0842	0.004881	0.028785	Monoclinic	
	Ag_5Te_3	22.901	0.9800	3,1,1	3.027	0.007272	0.019454	Hexagonal	

It has been observed that with the addition of Ag there is a slightly change in the peak position of Se_8 phase i.e 23.472° of $(\text{Se}_{80}\text{Te}_{20})_{99}\text{Ag}_1$, 18.472° of $(\text{Se}_{80}\text{Te}_{20})_{98}\text{Ag}_2$, 18.680° of $(\text{Se}_{80}\text{Te}_{20})_{97}\text{Ag}_3$ and 18.402° of $(\text{Se}_{80}\text{Te}_{20})_{96}\text{Ag}_4$ on 2θ axis. The value of the lattice parameters of the films annealed at 348K are $a = 15.018$, $b = 14.713$ and $c = 8.789$ give rise to the monoclinic structure with the space group $\text{P2}_1/\text{C}$. When the samples are annealed at the 398K, there is again slight change in the peak position of the Se_8 phase i.e 23.541° of $(\text{Se}_{80}\text{Te}_{20})_{99}\text{Ag}_1$, 18.611° of $(\text{Se}_{80}\text{Te}_{20})_{98}\text{Ag}_2$, 18.819° of $(\text{Se}_{80}\text{Te}_{20})_{97}\text{Ag}_3$ and 18.607° of $(\text{Se}_{80}\text{Te}_{20})_{96}\text{Ag}_4$ on 2θ axis with increase in the Ag content. The Se_8 phase having again the monoclinic structure with the lattice parameters $a = 9.054$, $b = 9.083$ and $c = 11.601$ with the space group $\text{P2}_1/\text{n}$. There is also the presence of the Ag_5Te_3 phase which also undergoes the change in the peak position from 29.236° to 22.891° with increasing Ag content. The Ag_5Te_3 phase having the hexagonal structure with the lattice parameters $a = 13.47$ and $c = 8.46$ with the space group $\text{P6}/\text{mmm}$. The particle size has been calculated by the Scherrer's formula [18].

$$D = \frac{0.9\lambda}{B \cos \theta} \quad (1)$$

where B represents the broadening of the diffraction lines measured at half its maximum intensity (radians) and D is the diameter of the crystal particle. The value of the particle radius obtained by the Scherrer's formulation is tabulated in Table 1.

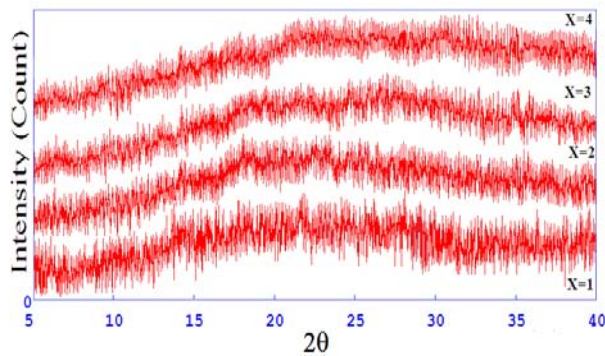


Fig.1 XRD pattern of a pristine $(\text{Se}_{80}\text{Te}_{20})_{100-x}\text{Ag}_x$ ($1 < x < 4$) bulk samples.

3.2 Calculation of activation energy of crystallization of $(\text{Se}_{80}\text{Te}_{20})_{100-x}\text{Ag}_x$ glassy samples by Piloyan–Borchardt method

The theoretical basis for interpreting the DSC data is provided by the formal theory of transforming kinetics given by Johnson-Mehl-Avrami formula [19]

$$\alpha_c = 1 - \exp[1 - (Kt)^n] \quad (2)$$

where α_c is a volume of the fraction crystallized and n be integer or half integer which depends on the mechanism of growth and the dimensions of the crystal [19, 20]. Here K

is reaction rate constant which has Arrhenius temperature dependence which is given by

$$K = K_0 \exp\left[\frac{-E_c}{RT}\right] \quad (3)$$

where E is the effective activation energy describing the overall crystallization process

$$E_G = \left(\frac{E_N + mE_c}{n}\right) \quad (4)$$

where E_N and E_G are the effective activation energies for nucleation and growth respectively, where $n=m$ for the nucleation frequency $I_v=0$ [21] and $n = m+1$ for $I_v \neq 0$ [19]. If E_N is negligible over the temperature range of concern in the thermoanalytical study [19], then

$$E_G = \frac{mE_c}{n} \quad (5)$$

Thus, the activation energy of growth (E_G) is

$$E_G = \frac{nE_c}{m} \quad (6)$$

There are different methods for the determination of the effective activation energy of the crystallization process. In non isothermal crystallization the relationship between the sample temperature T and the heating rate is given by

$$T = T_0 + \beta t \quad (7)$$

where T_0 is the initial temperature obtained by the extrapolation of the curve between temperature (T) and heating rate (β).

Differentiating the eq. 2 with respect to t, we get

$$\alpha_c' = (1 - \alpha_c)nK^n t^{n-1} \left[1 + \left(\frac{t}{K}\right)K'\right] \quad (8)$$

Here $\alpha_c' = \frac{d\alpha_c}{dt}$ and on taking the derivative of equation 3 with respect to t we get

$$K' = \frac{dK}{dt}, \text{ now rearranging the terms we get} \\ K' = \frac{dK}{dt} = \frac{dK}{dT} \frac{dT}{dt} K' = \frac{\beta EK}{RT^2} \quad (9)$$

Thus the equation (8) becomes

$$\alpha_c' = (1 - \alpha_c)nK^n t^{n-1} (1 + jt) \quad (10)$$

where $j = \frac{\beta E}{RT^2}$. If the value of T_0 in equation (7) is very small that it can be neglected then $T = \beta t$, then $jt \cong E/RT$, thus the above equation (10) becomes

$$\alpha_c' = (1 - \alpha_c)nK^n t^{n-1} \left(\frac{E}{RT}\right) \quad (11)$$

According to the Borchardt [22, 23], for $\alpha_c \ll 0.5$, the rate of reaction α_c' at a particular temperature T is proportional to the heat flow difference between the sample and the inert reference Δq . Thus we have

$$\alpha'_c = C\Delta q \quad (12)$$

Now deduced the value of t from equation 2

$$t^n = \frac{[1 - \ln(1 - \alpha'_c)]}{K} \quad (13)$$

Put the value of t in eq. (11)

$$\alpha'_c = (1 - \alpha_c)nK^{n-1}[1 - \ln(1 - \alpha_c)]^{\frac{n-1}{n}} \left(\frac{E}{RT}\right) \quad (14)$$

From equation (12)

$$C\Delta q = (1 - \alpha_c)nK^{n-1}[1 - \ln(1 - \alpha_c)]^{\frac{n-1}{n}} \left(\frac{E}{RT}\right) \quad (15)$$

Rearranging the above terms and taking the logarithm it yields

$$\ln\left(\frac{T\Delta q}{F(\alpha_c)}\right) = \ln\left[\frac{nK_o}{C}\right] + \ln\left[\frac{E}{R}\right] - \frac{E}{RT} \quad (16)$$

The method of Piloyan-Borchardt [24, 22] determines the variation of Δq (the heat flow difference between the sample and reference material) with temperature at constant heating rate. The determination of the complex activation energy of crystallization E_c can be made by using Piloyan's method [24]. This is based on the differential form of the model relation for α_c , and on Borchardt's assumption [22], that the reaction rate, $d\alpha_c/dt$, is proportional to inert reference, Δq , as detected by DSC. Thus, according to the equation

$$\ln\left(\frac{T\Delta q}{F(\alpha_c)}\right) = \ln\left(\frac{nE_c K_o}{RC}\right) - \frac{E_c}{RT} \quad (17)$$

$$F(\alpha_c) = (1 - \alpha_c)[-\ln(1 - \alpha_c)]^{\left(\frac{n-1}{n}\right)} \quad (18)$$

where $F(\alpha_c)$ is given as follows

The activation energy of crystallization E_c has been obtained by the slopes of the plots between $\ln(T\Delta q/F(\alpha_c))$ vs $1000/T$ (Fig. 2) for both phases. E_{c1} and E_{c2} stand for activation energy of crystallization for the first and second phase respectively. The value of activation energy of crystallization E_c obtained by Piloyan–Borchardt method for $(\text{Se}_{80}\text{Te}_{20})_{98}\text{Ag}_2$ at different heating rates is tabulated in Table 2, and the value of activation energy at different values of x at a heating rate of 10K/min is tabulated in Table 3.

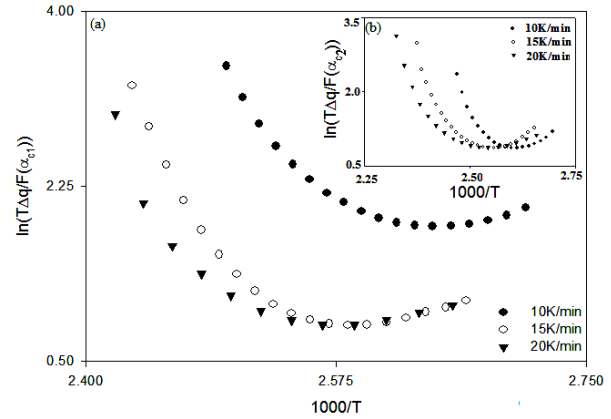


Fig. 2. The variation of $\ln(T\Delta q/F(\alpha_c))$ vs $1000/T$ for $(\text{Se}_{80}\text{Te}_{20})_{100-x}\text{Ag}_x$ ($x=2$) for first phase (a) and second phase (b) respectively at 10K/min.

Table 2. Activation energy of crystallization of $(\text{Se}_{80}\text{Te}_{20})_{98}\text{Ag}_2$ glassy system for both phase obtained by Piloyan-Borchardt method at different heating rates.

Heating rate (K/min)	$(\text{Se}_{80}\text{Te}_{20})_{98}\text{Ag}_2$	
	E_{c1}	E_{c2}
5	47.41	41.87
10	48.78	36.99
15	62.33	41.00
20	49.42	40.56

Table 3. The value of activation energy of crystallization (E_c) of $(\text{Se}_{80}\text{Te}_{20})_{100-x}\text{Ag}_x$ glassy system obtained by Piloyan - Borchardt method for both phases at heating rate of 10K/min

Composition	E_{c1}	E_{c2}
a- $(\text{Se}_{80}\text{Te}_{20})_{100}$	-	-
$(\text{Se}_{80}\text{Te}_{20})_{99}\text{Ag}_1$	48.30	36.86
$(\text{Se}_{80}\text{Te}_{20})_{98}\text{Ag}_2$	48.78	36.99
$(\text{Se}_{80}\text{Te}_{20})_{97}\text{Ag}_3$	49.07	37.89
$(\text{Se}_{80}\text{Te}_{20})_{96}\text{Ag}_4$	48.97	37.69

4. Discussion

Structural studies of $(\text{Se}_{80}\text{Te}_{20})_{100-x}\text{Ag}_x$ ($0 < x < 4$) bulk samples has been analysed by using the XRD data. The absences of the sharp peaks in the Fig.1 confirm the amorphous nature of the bulk samples. The XRD spectra of the bulk samples annealed at 348K confirms the formation of the Se_8 phase but the samples annealed at the 398K shows the presence of the Se_8 as well as Ag_5Te_3 phase, this is confirmed by the JCPDS-1998 data base.

The PDF files PDF#710528, PDF#761865 and PDF#471350 confirms the presence of the peaks of Se_8 (Monoclinic), Se_8 (Monoclinic), Ag_5Te_3 (Hexagonal) phase respectively. The presence of the monoclinic phases with the hexagonal phases represents the polycrystalline behaviours of the annealed bulk samples. The particle size has been calculated by the Scherrer's formula and found to be in the range of 0.008277 μm to 0.038694 μm . Activation energy of crystallization of glassy system for both phases has been obtained by Piloyan-Borchardt method at different x values as well at different heating rates. It has been observed that the value of activation energy of crystallization is highest for x= 3 and lowest for x= 1. The results show that the stability of sample is minimum for $(\text{Se}_{80}\text{Te}_{20})_{99}\text{Ag}_1$ and maximum for $(\text{Se}_{80}\text{Te}_{20})_{97}\text{Ag}_3$ among all the samples. The value of the activation energy of crystallization at different heating rates shows that the activation energy of crystallization is strongly temperature dependent.

5. Conclusion

The structural studies on the bulk samples of the $(\text{Se}_{80}\text{Te}_{20})_{100-x}\text{Ag}_x$ system and the applicability of the Piloyan-Borchardt method yield the following results.

1. All the pristine bulk samples are amorphous in the nature.
2. The particle size has been calculated by the Scherrer's formula and found to be in the range of 0.008277 μm to 0.038694 μm .
3. The value of activation energy of crystallization is highest for x= 3 and lowest for x= 1, which shows that the stability of sample is minimum for $(\text{Se}_{80}\text{Te}_{20})_{99}\text{Ag}_1$ and maximum for $(\text{Se}_{80}\text{Te}_{20})_{97}\text{Ag}_3$ among all the samples and the value of activation energy of crystallization at different heating rates shows that the activation energy of crystallization is strongly temperature dependent.

References

- [1] A. Onozuka, O. Oda, J. Non-Cryst Solids **103**, 289 (1988).
- [2] S. R. Elliot, Physics of amorphous materials, Longman publication, London (1991).
- [3] S. Fugimori, S. Sagi, H. Yamzaki, N. Funakoski, J. Appl. Phys. **64**, 100 (1988).
- [4] T. Katsuyama, S. Satoh, H. Matsumura, J Appl. Phys. **71**, 4132 (1992).
- [5] M. Asobe, Optical fiber technology **3**, 142 (1997).
- [6] T. Wagner, S. O. Kasap, J. Mater. Res. **12**, 1892 (1997).
- [7] K. Tanaka, Phys. Rev. B **39**, 1270 (1989).
- [8] K. Shimakawa, J. Non-Cryst. Sol. **77**, 1253 (1985).
- [9] J. Y. Shim, S. W. Park, H. K. Baik, Thin Solid Films **292**, 31 (1997).
- [10] J. M. Saitar, J. Ledru, A. Hamou, G. Saffarini, Physica B **245**, 256 (1998).
- [11] R. Chiba, N. Funakoshi, J. Non-Cryst. Sol. **105**, 149 (1988).
- [12] A. Bhargava, A. Williamson, Y. K. Vijay, I. P. Jain, J. Non-Cryst. Sol. **192**, 494 (1995).
- [13] R. M. Mehra, G. Kaur, A. Pundir, P.C. Mathur, Jpn. J. Appl. Phys. **32**, 128 (1993).
- [14] Z. Wang, C. Tu, Y. LI, Q. Chen, J. Non-Cryst. Sol. **191**, 132 (1995).
- [15] S. O. Kasap, T. Wagner, V. Aiyah, O. Krylouk, A. Bekirov, L. Tichy, J. Mat. Sci. **34**, 3779 (1999).
- [16] M. S. Kamboj, R. Thangaraj, Eur. Phys. J. Appl. Phys. **24**, 33 (2003).
- [17] D. Singh, S. Kumar, R. Thangaraj, J. Optoelectro. Adv. Mater. **12**, 1706 (2010).
- [18] B. D. Cullity, Elements of X-ray diffraction, Wesley Publishing Company Inc, London (1978).
- [19] H. Yinnon, D. R. Uhlmann, J. Non-Cryst. Solids. **54**, 253 (1983).
- [20] K. Matusita, S. Sakka, Phys. Chem. Glasses **20**, 81 (1979).
- [21] M. Kastner, D. Adler, H. Fritzsche, Phys. Rev. Lett. **37**, 1504 (1976).
- [22] H. J. Borchardt, J. Inorg. Nucl. Chem. **12**, 252 (1960).
- [23] M. A. Abdel-Rahim, M. M. Ibrahim, M. Dongol, A. Gaber, J. Mat. Sci. **27**, 4685 (1992).
- [24] G. O. Piloyan, I. D. Rybachikov, O. S. Novikov, Nature **212**, 1229 (1966).

*Corresponding author: rthangaraj@rediffmail.com